AD-A189 011 THE COMPLEX POINT SPREAD FUNCTION OF THE RSRE SAR (SYNTHETIC APERTURE RAD..(U) ROYAL SIGNALS AND RADAR ESTABLISHMENT MALVERN (ENGLAND) S P LUTTRELL SEP 87 1/1

UNCLASSIFIED RSRE-MEMO-4079 DRIC-BR-104823 F/G 17/9 NL

END
DATE FILMED
3-88
DTIC

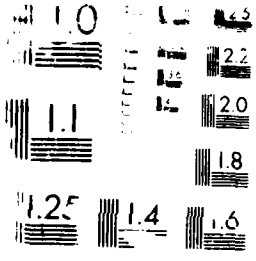
1.0
1.1
1.25
1.4
1.6
2.0
1.8

AD-A189 011

BR104023

DTIC FILE COPY

[illegible] No. 4079

ROYAL SIGNALS & RADAR ESTABLISHMENT

DTIC
S ELECTE D
FEB 0 3 1988

THE COMPLEX POINT SPREAD FUNCTION OF THE [illegible]

Author: [illegible]

[illegible]

ROYAL SIGNALS AND RADAR ESTABLISHMENT

Memorandum 4079

TITLE: THE COMPLEX POINT SPREAD FUNCTION OF THE RSRE SAR

AUTHOR: S P Luttrell

DATE: September 1987

SUMMARY

Super-resolution of SAR data requires that the complex point spread function (PSF) of the SAR be accurately known. We propose and implement a method of measuring the PSF which uses existing SAR images of targets as raw data. We find that in addition to the expected distortions of the azimuth response which arise from swing of the antenna and from artefacts of motion compensation processing, there are extensive and unexpected distortions of the range response. Most importantly the range response does not obey the principle of superposition (ie it is non-linear), and so SAR PSF calibration must be conducted with care. We estimate the complex SAR PSF when a bright target is present.

List of contents

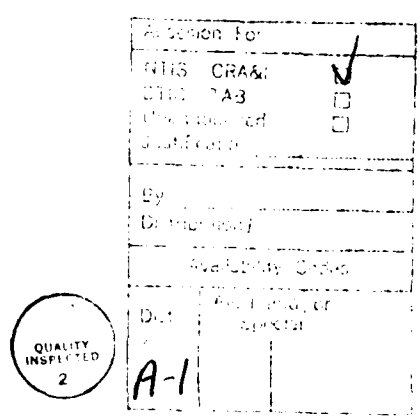

1. Introduction

The RSRE synthetic aperture radar (SAR) system is a fully coherent radar with an antenna length L = 1.9m operating at frequency ν = 10GHz (wavelength λ = 3cm). In operation the antenna is carried by an aircraft and is nominally pointed horizontally in a direction perpendicular to the aircraft's line of motion. Below we show the geometry which is relevant to operating the SAR system.

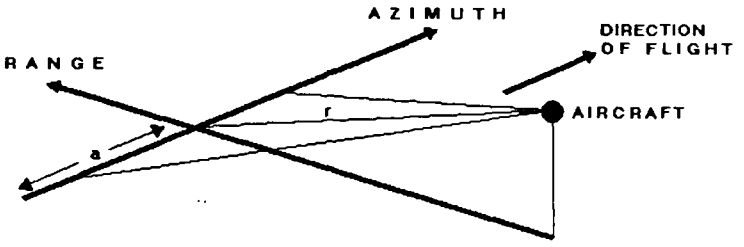

The azimuth direction is parallel to the nominal straight line along which the aircraft flies, and the range direction is perpendicular to this line. For a given range gate in the receiver the parameter r measures the actual range (ie slant range) from the antenna. Distance a in the azimuth direction is measured with respect to any convenient reference azimuth position.

Range resolution is provided by a chirp pulse compression system with a 100MHz bandwidth which ideally gives a range resolution of 1.5m assuming no weighting. In order to suppress range sidelobes Taylor weighting is imposed which reduces the effective chirp bandwidth and so correspondingly degrades the range resolution somewhat to approximately 2m. We shall see that in fact the range resolution is somewhat worse than this in practice, and that the range sidelobe structure is nothing like what we would expect.

Azimuth resolution is provided by coherently cross-correlating the returns in a single range gate with a reference function (ie matched filtering): this forms a synthetic aperture and corresponding synthetic beam. Ideally the resolution is then half the antenna length which is about 1m. Again, the antenna itself is weighted in order to reduce the real beam sidelobes so the achievable resolution is reduced somewhat.

In practice there are further causes of resolution degradation for both the range and azimuth directions. The range pulse compression system is not guaranteed to perform ideally since its

various component tolerances may drift after calibration, for instance. For azimuth resolution a serious problem is that naive matched filtering usually fails to form a compact synthetic beam, because the assumption that the aircraft flies in a straight line is incorrect. This problem has been the subject of many investigations which have culminated in a fully automatic data driven method of aircraft motion compensation [1]. A further problem for azimuth resolution is that the antenna is servoed to point perpendicular to the direction of aircraft motion, and so the real beam swings backwards and forwards in the range-azimuth plane. This modulates the returns on a time scale which is usually comparable with the synthetic aperture length, and so it can have a significant effect on the azimuth response.

The imagery which is obtained from the RSRE SAR after motion compensation is an excellent raw source of information for most image analysis packages. However any image analysis method which relies on detailed knowledge of the range and azimuth responses of the SAR can not so easily be applied. We refer in particular to super-resolution [2] which requires the complex valued point spread function (PSF) of the SAR as one of its inputs. Ideally we should process, with motion compensation, raw data which is derived from known point-like reflectors (eg corner cubes) which are placed on a weakly scattering background, but such data obtained under carefully controlled conditions is not available.

In this memorandum we demonstrate how the complex valued range response may be obtained, and we then attempt to obtain the azimuth response, although this is marred by the presence of antenna swing.

2. Point spread function theory

We shall first derive two alternative routes for obtaining information about a PSF from complex imagery. If we assume that the imaging system is linear and translation invariant (ie isoplanatic) then we may write the imaging equation as

$$g(x) = \int dy\ h(x-y)\ f(y) \tag{2.1}$$

where we have adopted a one-dimensional notation for simplicity, and where the various terms are defined as:

$$\begin{aligned} f(y) &= \text{complex scattered amplitude at position } y \\ g(x) &= \text{complex image amplitude at position } x \\ h(x-y) &= \text{complex PSF for separation } x-y \end{aligned} \tag{2.2}$$

Now consider two alternative types of f(y).

(1) Uncorrelated scattered amplitudes

$$\langle f(y_1) f^*(y_2) \rangle = E\ \delta(y_1-y_2) \tag{2.3}$$

The angle brackets denote an ensemble average, which is the same as a spatial average when the random process which generates the f(y) is stationary and ergodic. The correlation properties of g(x) are then

$$\begin{aligned} \langle g(x_1)g^*(x_2)\rangle &= \int dy_1 dy_2\ h(x_1-y_1)h^*(x_2-y_2)\langle f(y_1)f^*(y_2)\rangle \\ &= E\int dy\ h(x_1-y)h^*(x_2-y) \\ &= E\int dy\ h(y)\ h^*(x_2-x_1+y) \end{aligned} \qquad (2.4)$$

The ensemble average <..> may be replaced by a spatial average by a spatial average to yield

$$\langle g(x_1)g^*(x_2)\rangle \ \propto\ \int dx\ g(x)g^*(x_2-x_1+x) \qquad (2.5)$$

Combining equations (2.3) and (2.4) and Fourier transforming with respect to x_2-x_1 yields

$$|G(k)|^2 \ \propto\ |H(k)|^2 \qquad (2.6)$$

where k is spatial frequency, and G(k) and H(k) are the Fourier transforms of g(x) and h(x) respectively. The spatial power spectrum of an image of an uncorrelated stationary scattered field is thus equal (up to an unimportant constant factor) to the spatial power spectrum of the PSF.

This result may be used to obtain $|H(k)|^2$ for the SAR by Fourier transforming SAR images of featureless regions of "pure speckle" : these correspond the assumptions which we made about f(y) in equation (2.3)

(2) Point source of scattered amplitude

Such a source at position y=0 is represented as

$$f(y) = A\ \delta(y) \qquad (2.7)$$

which gives an image

$$\begin{aligned} g(x) &= \int dy\ T(x-y)\ A\ \delta(y) \\ &= A\ T(x) \end{aligned} \qquad (2.8)$$

Thus a point target gives rise to an image which is trivially proportional to the PSF which we wish to determine.

The conditions under which SAR data are collected make it impossible to find isolated point targets which satisfy equation (2.7) exactly, because they are invariably surrounded by clutter, and so at best f(y) has the form

$$f(y) = A\ \delta(y) + f_o(y) \qquad (2.9)$$

The best that we can attempt to do is to seek point-like targets which have a large amplitude A in the hope that the $A\delta(y)$ term dominates the $f_o(y)$ term in equation (2.9).

This analysis has been expressed in one dimension only. For the (two-dimensional) SAR it is a very good approximation to factorise the PSF and its Fourier transform into range and azimuth parts thus

$$H(\underline{k}) = H(k_r, k_a) = R(k_r)\, A(k_a) \qquad (2.10)$$

where $R(k_r)$ and $A(k_a)$ are the spatial Fourier transforms of the range and azimuth factors respectively. This approximation becomes invalid when "range walk" occurs, but such conditions do not occur for the RSRE SAR so we shall assume PSF factorisation.

A prescription for determining the SAR PSF which is suggested by the above analysis to obtain the spatial power spectrum $|H(\underline{k})|^2$ from regions of pure speckle: such data is plentiful so the statistical errors will be small. Following this the phase $\arg(H(\underline{k}))$ of the Fourier transform $H(\underline{k})$ of the PSF could be obtained from point-like target data: this would place the least possible reliance on the (somewhat suspect) point-target data. However we assumed that the PSF was translation invariant which is very good approximation only for the range direction because the characteristic drift time of the range response is very long, and so we may determine $R(k_r)$ using the above analysis. The azimuth response is not translationally invariant because of the effects of antenna swing, which makes this approach to determining $A(k_a)$ somewhat questionable.

3. Point spread function extraction

The raw data which we used to determine the PSF was derived from SAR tape number 35. The header block contained the following information:

Date of flight:	12 April 1984
Altitude:	27000 feet
Nominal range:	35 kilometers
Nominal velocity:	200 feet/second
Area imaged:	Salisbury plain (Larkhill)

We first surveyed the entire tape at a 24 metre linear resolution to localise regions of interest (see Figure 1). Note that this image does not need to be autofocussed because we are interested only in discovering roughly where regions of pure Gaussian speckle and regions containing point-like targets are located. In Figure 2 we present a montage of 25 autofocussed 32x32 high resolution images (1.5 metres linear resolution) of regions which were selected from the low resolution image in Figure 1 as containing likely point targets. Clearly most of these images have a complicated structure at high resolution and so must be

rejected from the PSF analysis. This leaves only images 1, 2 and 12 from Figure 2 as good candidates, and we show these as 64x64 high resolution images in Figure 3. These comprise our raw target data from which we intend to extract the SAR PSF.

The first step in the analysis is to preprocess the complex target data so as to centre the peak of the target image on the (0,0) pixel of the image. This will ensure that the Fourier transform has no artificial linear phase gradient present. We achieve this by sinc interpolating the 64x64 complex images onto a 256x256 image in order to subsample the complex data, and then register the peak in each 256x256 image with the (0,0) pixel. We then invert the sinc interpolation to recover the correctly centred 64x64 complex image. Target image 12 contains two targets, so we generate two images, one with each target correctly centred. We shall henceforth refer to targets 1, 2, 12.1 (upper-left) and 12.2 (lower right) as targets 1, 2, 3 and 4 respectively. We also adjust the phase of each 64x64 image globally to ensure that the phase of the (0,0) pixel is the same in each case; we arbitrarily choose zero phase.

We wish to obtain an estimate of the Fourier transform $H(\underline{k})=R(k_r)A(k_a)$ (see equation (2.10)) of the SAR PSF from this target data. However the target images have two principal components: target and clutter. The clutter contribution to the Fourier transform is incoherent and thus will degrade the coherent target contribution, so we must eliminate it as far as possible. This is easily achieved by masking out the clutter in the image in such a way that we can be sure that the clutter is substantially removed, whilst the target is substantially preserved. We therefore use a mask which has the form shown below, where the black area (except the border) transmits and the white areas do not transmit.

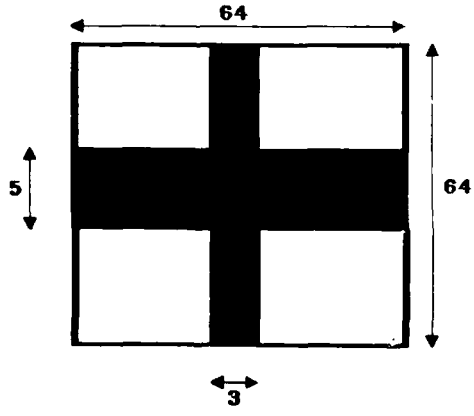

The dimensions shown are in units of pixel separation. The cross is centred on the (0,0) pixel (ie on the target). The 3 pixel wide vertical stripe encompasses virtually all of the azimuth factor of the SAR PSF, and the 5 pixel wide horizontal stripe does the same for the range factor. The overall effect of the cross is to reject clutter.

In Figure 4 we show the modulus of the Fourier transform of each masked complex target image. In Figure 5 we show the phase of these Fourier transforms, where $-\pi$ is coded as black and $+\pi$ is coded as white. Targets 1-4 are found in the top-left, top-right, bottom-left and bottom-right positions in Figures 4 and 5. When viewing Figures 4 and 5 keep in mind that they are good approximations to the Fourier transform $H(\underline{k})$ of the SAR PSF. Figure 4 reveals that the range component $R(k_r)$ of $H(\underline{k})$ is displaced from the origin, and so we may immediately deduce that there is an anomalous range phase gradient produced somewhere in the SAR system; this does not affect image quality of course. The most important property of $H(\underline{k})$ which is revealed by Figures 4 and 5 is the approximate constancy of the modulus and phase of the azimuth component $A(k_a)$ with respect to k_a, so we may recover a good estimate of the range component $R(k_r)$ by averaging the Fourier transform of the complex target data over k_a.

The modulus of the Fourier transform averaged over azimuth is shown for targets 1 and 2 in Figure 6, and for targets 3 and 4 in Figure 7. The corresponding phases are shown in Figures 8 and 9. The moduli are displayed on a scale which ranges from zero to the maximum modulus in each case. The phases are displayed in the range $[-\pi,+\pi]$. The principal feature of Figures 6 and 7 is the very strong sawtooth component. This is not a design feature of the SAR system, which is nominally has a Taylor weighted envelope engineered into the SAW pulse compression filter. The exact source of this sawtooth is not clear, but clearly the SAR system is faulty. This problem is not too severe because the effect of the sawtooth can be accounted for by calibrating the PSF as we are attempting to do. The effect of the sawtooth on the SAR PSF is clear; it acts as a diffraction grating which produces anomalous sidelobes in the range direction. These are clearly visible in Figure 3. The principal feature of Figures 8 and 9 is phase stationarity in the region where the modulus is greatest, and the wild fluctuations of phase in the regions where the modulus is smallest. The small perturabations about zero phase seem to be correlated with the sawtooth component of the modulus. The wild fluctuations of phase arise because when the modulus is small we approach the zeros of the complex Fourier transform where phase must vary rapidly.

In Figure 10 we show the modulus and phase of the average of the complex Fourier transforms corresponding to Figures 6-9. The averaging process cleans up the modulus somewhat, and it reveals that the small phase perturbations combine constructively to produce a result which is clearly correlated with the sawtooth.

We now use this best estimate of $R(k_r)$ to remove $\arg(R(k_r))$ from the complex Fourier transforms of the target data, and then average the resulting phase-compensated complex Fourier transforms in the range direction. This procedure gives a good estimate of $A(k_a)$ because the absence of range phase variation ensures that the average in the range direction consists of constructively interfering components. In Figures 11 and 12 we show the moduli of this average for targets 1-4, and in Figures 13 and 14 we show the corresponding phases. The moduli are displayed in the range zero to the maximum modulus in each case, and the phase is displayed in the range $[-\pi,+\pi]$. In Figures 13 and 14 note how the phase is very close to zero except at the very edge of the band; this indicates that the autofocussing process is performing well. In Figure 15 we show the average of the complex Fourier transforms corresponding to Figures 11-14. The precise form of the modulus in Figure 15 is affected by the real beam envelope, any residual clutter passed by the mask, the precise details of the autofocussing program, and it could be degraded by averaging over targets for which the antenna was pointing in different directions. The phase in Figure 15 departs from its constant value at the ends of the band, and we see from Figures 13 and 14 that this trend is mostly systematic. The most likely explanation for this effect is that the phase of a point target as it sweeps through the beam has a quartic component which dominates at the edge of the beam. This translates into a systematic departure of the phase of $A(k_a)$ at the edge of the band in high resolution images (which use a substantial fraction of the real beam width). Another problem which may arise is aliassing which can occur when phase compensation terms are introduced into the data (by the SAR processing program) without modifying the sampling scheme; this can lead to a small amount of overspill at the ends of the band under typical conditions. All of the problems discussed in this paragraph make the results in Figure 15 suspect.

In an attempt to obtain better estimates of $|R(k_r)|$ and $|A(k_a)|$ we now examine the modulus of the Fourier transform of pure speckle (see equation (2.6)). In order to compare these results with the estimates above from target data we selected 8 256x256 images containing pure speckle (as far as we could tell by eye). We then split each such image into 16 64x64 subimages, and averaged the modulus of the Fourier transform of all the 64x64 subimages obtained from one 256x256 image. We hope that each 256x256 image is not affected too badly by antenna swing, and that therefore the averaging process does not smear the modulus. The safety margin for this assumption is that the antenna swings by much less than a beamwidth (<1 degree) in the time it takes to move 256 pixels (400 metres, or 2 seconds). A better averaging scheme (which we have not attempted here) would be to select the 64x64 speckle images from the same azimuth position, thus absolutely minimising the effect of antenna swing. The averaged results for $|R(k_r)|$ and $|A(k_a)|$ for each of the 8 256x256 speckle images is shown in Figures 16-23. $|R(k_r)|$ is highly reproducible as we expect, but $|A(k_a)|$ reveals that the antenna is pointing in different directions for each of the 8 speckle images. In Figure 24 we show the average of Figures 16-23 which cleans up the estimate of $|R(k_r)|$ somewhat, but smears the estimate of $|A(k_a)|$ because of antenna swing.

The most important result which we obtain from Figure 24 is that $|R(k_r)|$ is NOT the same as the corresponding result obtained from target data in Figure 10: this is a complete surprise! We

have carefully checked that the minimum and maximum values on the modulus displays are what we think they are. Although the general structure of $|R(k_r)|$ is similar there are two obvious differences. Firstly, the background "pedestal" is relatively much weaker for the target than for speckle. Secondly, the relative depth of modulation of the sawtooth is much greater for the target than for speckle, although the peaks and troughs of the sawtooth are located in the same places. The conclusion is unavoidable: the SAR PSF does NOT obey the principle of superposition (ie it is non-linear). Thus any calibration of the SAR PSF much be performed under the conditions in which subsequent image analysis is to be attempted. For instance, super-resolution analyses the images of targets, so it would be inappropriate to use an $|R(k_r)|$ which is obtained from speckle images. The precise cause of this non-linearity is not known at present, but it would be highly desirable to remove it because it complicates the detailed analysis of SAR images.

All previous studies have assumed that the RSRE SAR PSF obeys superposition (ie is linear); consequently studies which attempt to relate the SAR image to a cause (ie cross section) using a fixed PSF might lead to incorrect conclusions about the relative strength of weak and strong components of the cross section. In particular the higher moments (but not the lower moments) of a cross section depend strongly on its target-like component, so the relative sizes of deduced high and low moments of a cross section are likely to be in error due to the non-linearity of the SAR PSF.

A further minor observation is the small peak in $|R(k_r)|$ at the lower limit of the band in Figure 24. This is caused by an error in the program which transposes the original raw data into a form suitable for processing into an image. This error (which has since been rectified) occasionally introduces into the data an almost periodic component at the Nyquist frequency in the range direction; this leads directly to the anomalous peak which we observe.

Because we are interested in the SAR PSF for targets we must discard all of the speckle results for $|R(k_r)|$ (Figures 16-24) because of the non-linearity problem. A caveat that remains with $A(k_a)$ is the possibility still of antenna swing corrupting the results.

We present the modulus and phase of the estimated complex Fourier transform of the SAR PSF (determined using Figures 10 and 15) in Figure 25, and the modulus of the 4 times sinc interpolated PSF in Figure 26. This is the best estimate of the non-linear SAR PSF (in the target regime) which we can construct at present. A minor improvement would be possible by unfolding the effects of antenna swing, but we do not consider the improvement to be currently worth the effort.

4. Discussion and conclusions

This work is necessary because of a pressing need for an accurate calibration of the RSRE SAR PSF for use in super-resolution work, and because there is no possibility that a rigorous calibration of the SAR under controlled conditions will be performed in the forseeable future. Although the method that we have used has undesirable sources of error such as clutter contamination of targets and antenna swing smearing, it is nevertheless the only realistic choice open to us.

One potential output parameter from motion compensation processing is the point direction of the real beam in the range-azimuth plane, which we could be used to correct the azimuth data to remove some of the effects of antenna swing. However the ideal solution is simply to servo the antenna so that it always points perpendicular to some nominal line of flight; the need for antenna swing compensation would then be removed.

We find that the SAR does not obey the principle of superposition (ie it is non-linear) because it responds in different ways to (weak) clutter and to (strong) targets. This prevents us from combining the target and clutter results when determining the PSF. Such non-linearity also raises a question mark over the comparison of targets and clutter which are reconstructed from SAR images. In the language of moments, is it valid to compare low order and high order reconstructed moments? These are open questions at present, and PSF-sensitive predictions should be reassessed in the light of our discovery.

The PSF results from targets are consistent enough for us to present an estimate of the SAR PSF (Figure 26). This PSF shows unexpected diffraction peaks in the range direction; these arise from a sawtooth component in the Fourier transform of the range response. This is a fault in the SAR system which should be rectified, although image processing techniques could be used to remove its effect.

On inspection of Figure 26 the range resolution is clearly much worse than the azimuth resolution. This PSF is obtained using target (not clutter) data, and so the high spatial frequencies in the range direction are suppressed somewhat relative to those for clutter. Comparing Figures 10 and 15 reveals that the bandwidth in the range direction is only about 1/3 of that in the azimuth direction (which is nominally full band). The PSF in Figure 26 thus has an azimuth resolution ≈1.5 metre and a range resolution ≈4-5 metre. Any estimate of the range resolution which is obtained using a global measure such as an image autocorrelation function will be sensitive principally to the range bandwidth shown in Figure 24, which leads to a much better range resolution than Figure 10. Such an estimate is clearly inappropriate if the resolution criterion is then applied to targets.

We intend to use the SAR PSF calibrated from target data in super-resolution studies of RSRE SAR data: results will be presented in the future.

Acknowlegements

We thank T M Mason and Dr J W Wood for useful discussions during the course of this work.

References

[1] Finley I P and Wood J W, 1985, RSRE memo 3790, "An investigation of SAR autofocus".

[2] Luttrell S P, 1985, RSRE memo 3785, "A super-resolution model for SAR".

Figure captions

Figure 1: Low resolution image (24 metre linear pixel size) of SAR tape 35.

Figure 2: Montage of high resolution images (1.5 metre linear pixel size) of 25 possible targets extracted from Figure 1.

Figure 3: 64x64 high resolution images of 3 candidate point target images (1, 2 and 12) extracted from Figure 2.

Figure 4: Moduli of Fourier transforms of targets in Figure 3. See the text for a more detailed discussion.

Figure 5: Phases of Fourier transforms corresponding to Figure 4.

Figure 6 and
Figure 7: Moduli of range Fourier transforms of targets in Figure 3 obtained by coherent azimuth averaging.

Figure 8 and
Figure 9: Phases of range Fourier transforms corresponding to Figures 6 and 7.

Figure 10: Modulus and phase of average cf range Fourier transforms obtained from Figures 6-9.

Figure 11 and
Figure 12: Moduli of azimuth Fourier transforms of targets in Figure 3 obtained by coherent range averaging after range phase correction. See the text for a more detailed discussion.

Figure 13 and
Figure 14: Phases of azimuth Fourier transforms corresponding to Figures 11 and 12.

Figure 15: Modulus and phase of average of azimuth Fourier transforms obtained from Figures 11-15.

Figures 16-23:
Moduli of range and azimuth Fourier transforms each obtained from a modulus average of 8 64x64 Fourier transforms of pure speckle.

Figure 24: Moduli of range and azimuth Fourier transforms obtained by averaging Figures 16-23.

Figure 25: Modulus and phase of estimated Fourier transform obtained from Figures 10 and 15.

Figure 26: Modulus of estimated SAR point spread function.

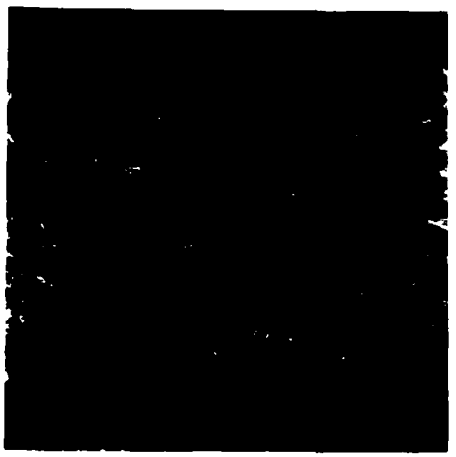

Figure 1

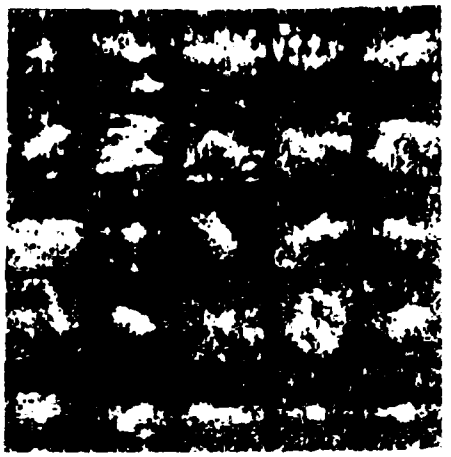

Figure 2

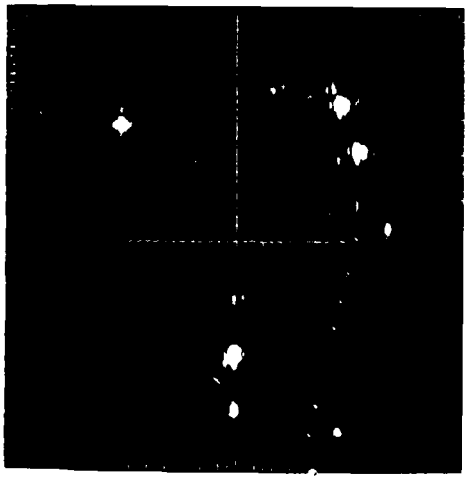

Figure 3

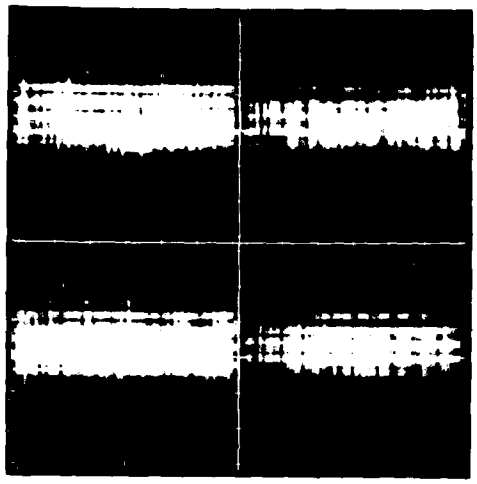

Figure 4

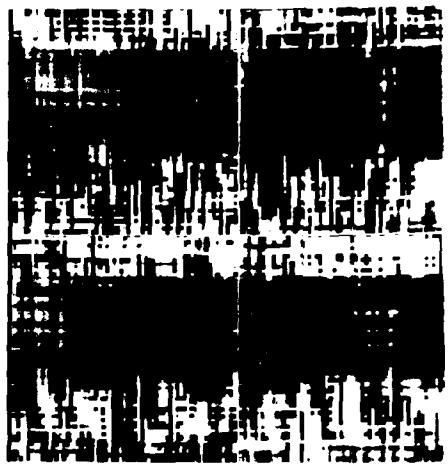

Figure 5

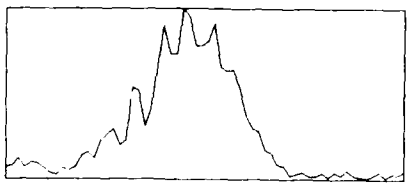

Figure 6

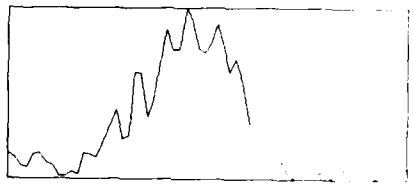

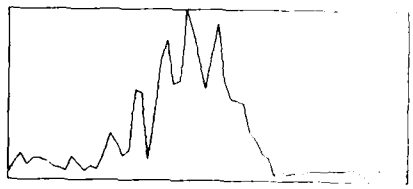

Figure 7

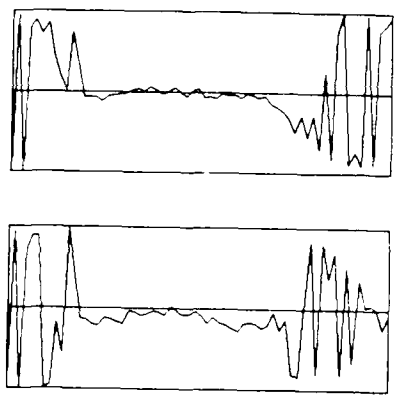

Figure 8

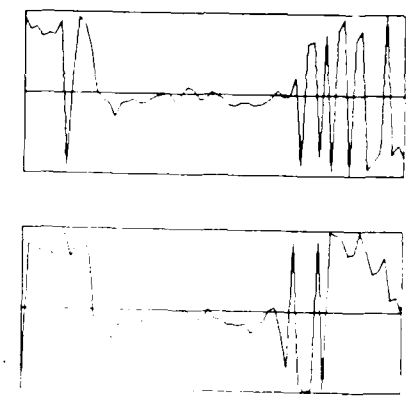

Figure 9

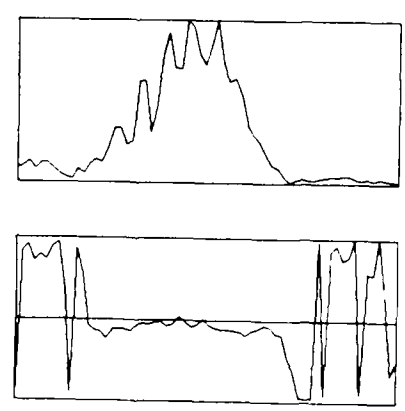

Figure 10

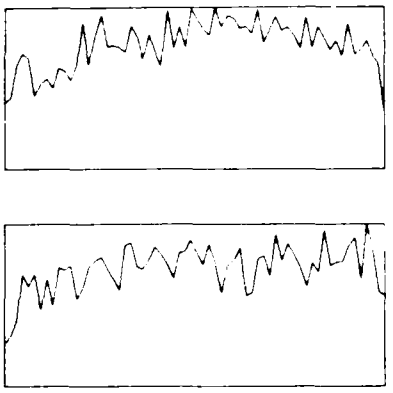

Figure 11

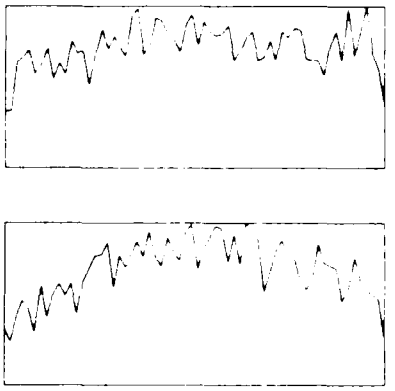

Figure 12

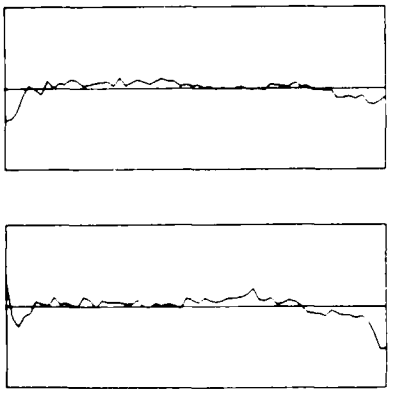

Figure 13

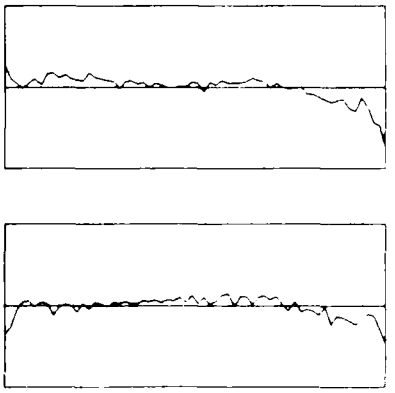

Figure 14

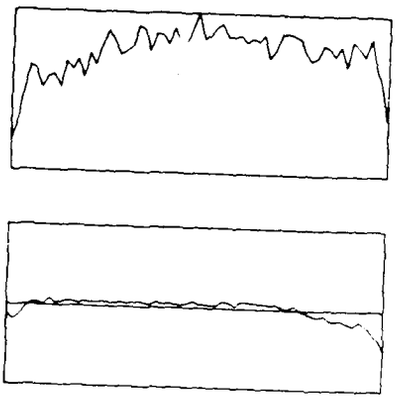

Figure 15

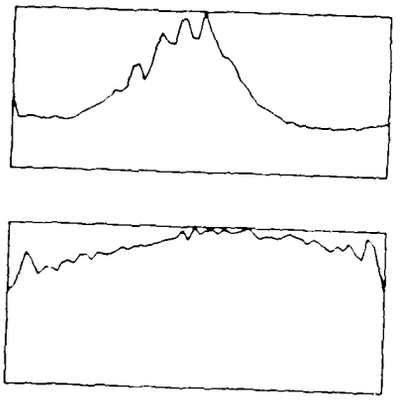

Figure 16

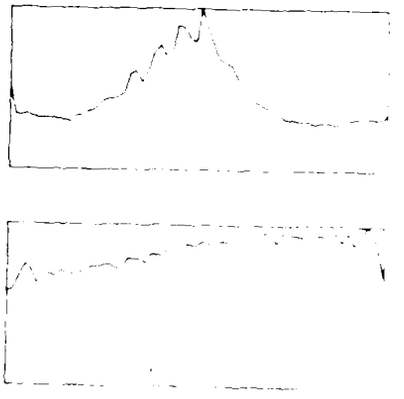

Figure 17

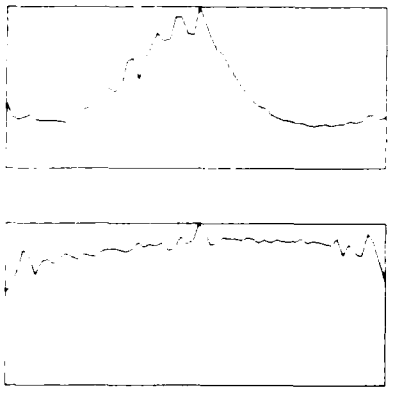

Figure 18

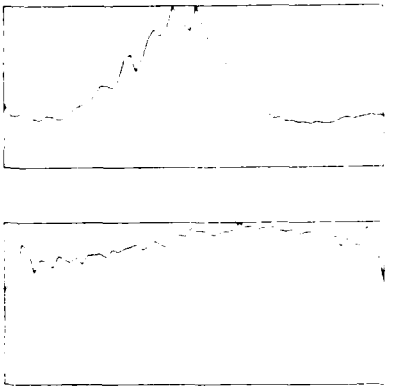

Figure 19

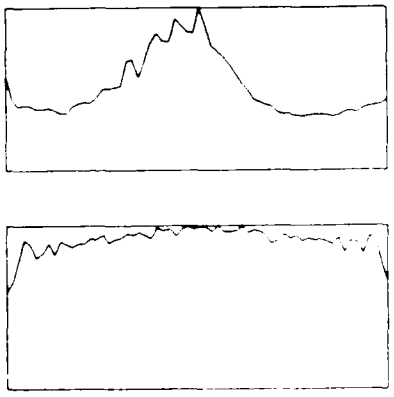

Figure 20

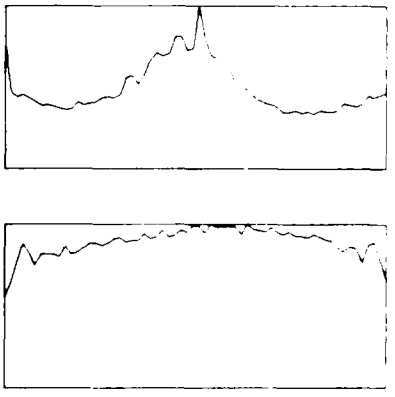

Figure 21

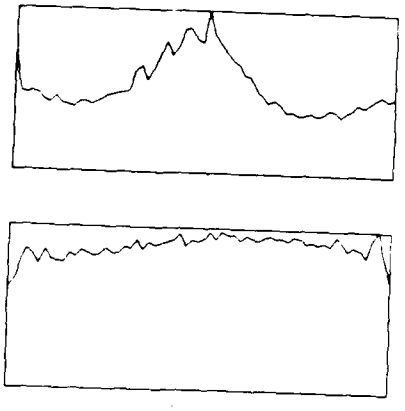

Figure 22

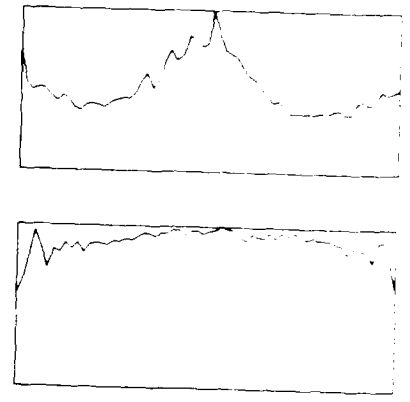

Figure 23

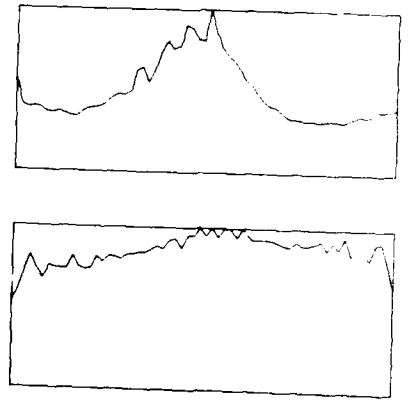

Figure 24

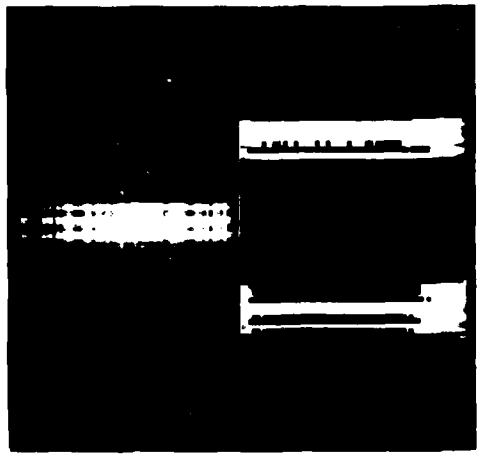

Figure 25

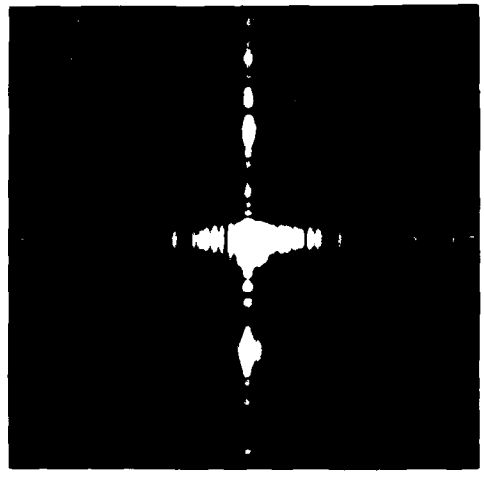

Figure 26

DOCUMENT CONTROL SHEET

Overall security classification of sheet ..... UNLIMITED .....

(As far as possible this sheet should contain only unclassified information. If it is necessary to enter classified information, the box concerned must be marked to indicate the classification eg (R) (C) or (S)

1. DRIC Reference (if known)	2. Originator's Reference MEMO 4079	3. Agency Reference	4. Report Security Classification UNLIMITED
5. Originator's Code (if known) 778400	6. Originator (Corporate Author) Name and Location RSRE, St Andrews Road, Malvern, Worcs. WR14 3PS		
5a. Sponsoring Agency's Code (if known)	6a. Sponsoring Agency (Contract Authority) Name and Location		

7. Title COMPLEX POINT SPREAD FUNCTION OF THE RSRE SAR

7a. Title in Foreign Language (in the case of translations)

7b. Presented at (for conference papers) Title, place and date of conference

8. Author 1 Surname, initials	9(a) Author 2	9(b) Authors 3,4...	10. Date	pp ref
LUTTRELL, S.P.			1987.09	21

11. Contract Number	12. Period	13. Project	14. Other Reference

15. Distribution statement

Descriptors (or keywords)

continue on separate piece of paper

Abstract Super-resolution of SAR data requires that the complex point spread function (PSF) of the SAR be accurately known. We propose and implement a method of measuring the PSF which uses existing SAR images of targets as raw data. We find that in addition to the expected distortions of the azimuth response which arise from swing of the antenna and from artefacts of motion compensation processing, there are extensive and unexpected distortions of the range response. Most importantly the range response does not obey the principle of superposition (ie it is non-linear), and so SAR PSF calibration must be conducted with care. We estimate the complex SAR PSF when a bright target is present.

END

DATE
FILMED

3 88

DTIC